Available online at www.sciencedirect.com
SCIENCE DIRECT®
Journal of Sound and Vibration 285 (2005) 597–614
JOURNAL OF SOUND AND VIBRATION
www.elsevier.com/locate/jsvi

Vibration and dynamic stability of a traveling sandwich beam

Wen-Pei Yang[a], Lien-Wen Chen[a,*], Ching-Cheng Wang[b]

[a]*Department of Mechanical Engineering, National Cheng Kung University, Tainan 70101, Taiwan, ROC*
[b]*Institute of Manufacturing Engineering, National Cheng Kung University, Tainan 70101, Taiwan, ROC*

Received 3 June 2003; received in revised form 30 March 2004; accepted 26 August 2004
Available online 15 December 2004

Abstract

The vibration and dynamic stability of a traveling sandwich beam are studied using the finite element method. The damping layer is assumed to be linear viscoelastic and almost incompressible. The extensional and shear moduli of the viscoelastic material are characterized by complex quantities. Complex-eigenvalue problems are solved by the state-space method, and the natural frequencies and modal loss factors of the composite beam are extracted. The effects of stiffness and thickness ratio of the viscoelastic and constrained layers on natural frequencies and modal loss factors are reported. Tension fluctuations are the dominant source of excitation in a traveling sandwich material, and the regions of dynamic instability are determined by modified Bolotin's method. Numerical results show that the constrained damping layer stabilizes the traveling sandwich beam.

1. Introduction

In order to reduce vibration-induced stress and displacement amplitudes in structures, the use of thin constrained damping layers has become common practice in many industries. In three-layered damped sandwich beams, the viscoelastic material undergoes considerable shear strain as the structure bends, dissipating energy and attenuating vibration response. The damping property of a sandwich beam with a viscoelastic core is usually expressed as the modal loss factor for the corresponding vibration mode.

*Corresponding author. Fax: +886 6 2352973.
E-mail address: chenlw@mail.ncku.edu.tw (L.-W. Chen).

0022-460X/$ - see front matter © 2004 Elsevier Ltd. All rights reserved.
doi:10.1016/j.jsv.2004.08.018

Nomenclature

b	the width of the traveling beam
c	axial moving speed of the traveling beam
$\tilde{c}$	$\sqrt{12\rho_3 L^2/E_3 h_3^2} \times c$, non-dimensional axial moving speed
$\mathbf{D}_i$	the transverse thickness interpolation matrix for Layer i
E_i	the Young's modulus of Layer i, $i = 1, 2, 3$
G_i	the effective shear modulus of Layer i, $i = 1, 2, 3$
$G_{v,2}$	the shear modulus of the viscoelastic material
h_i	thickness of Layer i, $i = 1, 2, 3$
$\tilde{h}_i$	h_i/h_3, non-dimensional thickness of Layer i, $i = 1, 2$
L	length of the traveling beam
L_e	length of the element
$N(x)$	the longitudinal thickness interpolation matrix for Layer i
P	external tension
P_o	static component of the external tension
P_t	dynamic component of the external tension
u, w	axial and transverse displacement
$\mathbf{U}_i^e$	the nodal displacement vector of the element e in Layer i
ρ	the density of the traveling beam
η	the loss factor of the viscoelastic material
Θ	frequency of the external tension
$\tilde{\Theta}$	$\Theta L^2/\sqrt{E_3 h_3^2/12\rho_3}$, non-dimensional frequency of the external tension
ω	the natural frequency of the traveling sandwich beam
$\tilde{\omega}$	$\omega L^2/\sqrt{E_3 h_3^2/12\rho_3}$, non-dimensional natural frequency of the beam

Many authors have proposed analytical techniques that predict the performance of beams or plates with constrained layers. Earlier theoretical works to sandwich structures with a viscoelastic core could be traced back to Kerwin [1], Ross et al. [2], and Di Taranto [3]. They presented the fourth- and sixth-order theories for the axial and bending vibrations of beams. Then, Mead and Markus [4] refined and extended the theory of Di Taranto and treated beams with arbitrary boundary conditions. The refined theory assumed that the upper layer bent in the transverse direction exactly as the lower one and that the viscoelastic layer underwent pure shear and did not change its thickness under deformation. Yan and Dowell [5] and Rao and He [6] adopted the model of Mead and Markus to study the damping mechanism of the viscoelastic layer and Rao [7] reformulated the sixth-order theory by an energy approach.

While the above efforts focused on analytical solutions of the viscoelastic sandwich beam, others have developed finite element techniques to evaluate the performance of the damped structure of constrained layers. Finite element models offer structural analysts the ability to model various boundary conditions, complex loadings and non-uniform features such as material discontinuities and point masses. By taking advantage of the finite element model, Johnson et al. [8] have developed a three-dimensional model using the MSC/NASTRAN® computer program. They discussed the harmonically excited vibration of a sandwich beam. Zapfe and Lesieutre [9] proposed the discrete layer finite element (DLFE) model for the dynamic analysis of composite sandwich beams with integral damping layers. The DLFE model is free from the effects of shear locking, includes both transverse and rotatory inertia and automatically enforces displacement continuity at layer interfaces.

When a structure is subjected to axial periodic loads, the forced response becomes dynamically unstable under certain circumstances. Such an induced violent vibration is called

the dynamic instability or parametric resonance. Bolotin [10] and Evan-Iwanowski [11] reported comprehensive studies for the dynamic instability of mechanical components. The Mathieu–Hill equation [10,12] is obtained while resolving the parametric vibration of a beam that is subjected to a compressive dynamic force. The dynamic instability problems of a viscoelastic structure have been widely investigated. Stevens [13] discussed the dynamic stability of an initially straight, simply supported viscoelastic column subjected to a harmonically varying axial load under the assumption that the simple spring-dashpot model adequately represents a viscoelastic column material. The effects of the viscoelastic material behavior on the dynamic instability of a viscoelastic column were studied both analytically and experimentally by Stevens and Evan-Iwanowski [14]. Dost and Glockner [15] investigated the dynamic stability of simply supported perfect columns made of a linearly viscoelastic material and subjected to an axial periodic load. The solution of the integro-differential equation was obtained by means of Laplace transforms. All the above vibration analyses consider dynamic instability problems of stationary structures.

Reducing the vibration in an axially moving structure is an important engineering problem in areas of chemical, textile, computer, and tape recorder industries. Wickert and Mote [16] first reviewed literatures on the vibration and dynamic stability of axially moving structures. Then, they investigated the transverse vibrations of traveling strings and beams, and found the general solution of the system through modal analysis and Green's function method [17]. They further presented the solutions of an axially accelerating structure by the method of state space and Rayleigh's quotient, where the relation between frequencies and transport speeds of a moving string was obtained [18]. For a belt driven by pulleys, the parametric excitations are primarily caused by the belt defects and the torque pulses generated in the driving mechanics. Then, the parametric instability in a traveling sandwich beam is also considered.

The vibration analysis and dynamic instability problems of a traveling beam with a constrained viscoelastic layer are investigated in the present studies. The traveling beam is assumed to be simply supported at both ends and moving at a constant velocity. The DLFE model is adopted to derive the finite element equations of motion for the three-layer composite beam. The extensional shear moduli of the linear isotropic viscoelastic material layer are described by the complex quantities. The effects of modulus ratio, and thickness of constrained layer and the viscoelastic core layer on the natural frequencies and modal loss factors of an axial moving sandwich beam are studied. Thereby, the dynamic stability problems of a traveling sandwich beam are solved. Bolotin's method is applied to determine the regions of dynamic instability of the Mathieu–Hill equation with complex coefficients. The eigenvalue problems are then solved by the modified complex eigensolution method. The influences of various parameters on the dynamic stability of the traveling beam with a constrained damping layer treatment are also investigated.

The rest of this paper consists of three sections. Section 2 presents the finite element formulation, where discrete layer finite element, strain–displacement relation, kinetic and strain energies, equations of motion, free vibration, and dynamic stability are addressed in the stated order. The proposed method is implemented and results including characteristics affecting the primary dynamic stability region are presented in Section 3. Section 4 contains the conclusion.

2. Finite element formulation

A sandwich beam traveling at a constant velocity c with tension P is considered. The beam travels between two pulleys, which are separated by a distance L as shown in Fig. 1. The constrained damping layer consists of two layers. The upper layer, designated as Layer 1, is a pure elastic, isotropic and homogeneous constraining layer, and the middle layer, designated as Layer 2, is the linear viscoelastic material layer. Layer 2 is capable of dissipating vibratory motions. The host beam, designated as Layer 3, is assumed to be undamped, isotropic and homogeneous. The thicknesses of Layer 1, 2, and 3 are h_1, h_2, and h_3, respectively, and perfect bonding at interfaces between layers is assumed.

2.1. DLFE

The DLFE of Fig. 2(a) is adopted, where the beam element of length L_e and thickness h_i of Layer i has seven degrees of freedom. They are displacements in the x direction, U_i^A, U_{i+1}^A, U_i^B and U_{i+1}^B, and transverse displacements, W_i^A, W_i^B, and W_i^C. Fig. 2(b) shows the nodal degrees of freedom for finite elements of Layer 1–3. Let $w_i(x,t)$ be the transverse displacement of Layer i at (x,t). Assume that the transverse displacements are constant through the beam thickness. Then, the transverse normal strain is zero. In addition, values of W_i^A, W_i^B, W_i^C, and $w_i(x,t)$ remain the same for all Layers 1–3. Therefore, the subscript i of W_i^A, W_i^B, W_i^C, and $w_i(x,t)$ is dropped hereafter.

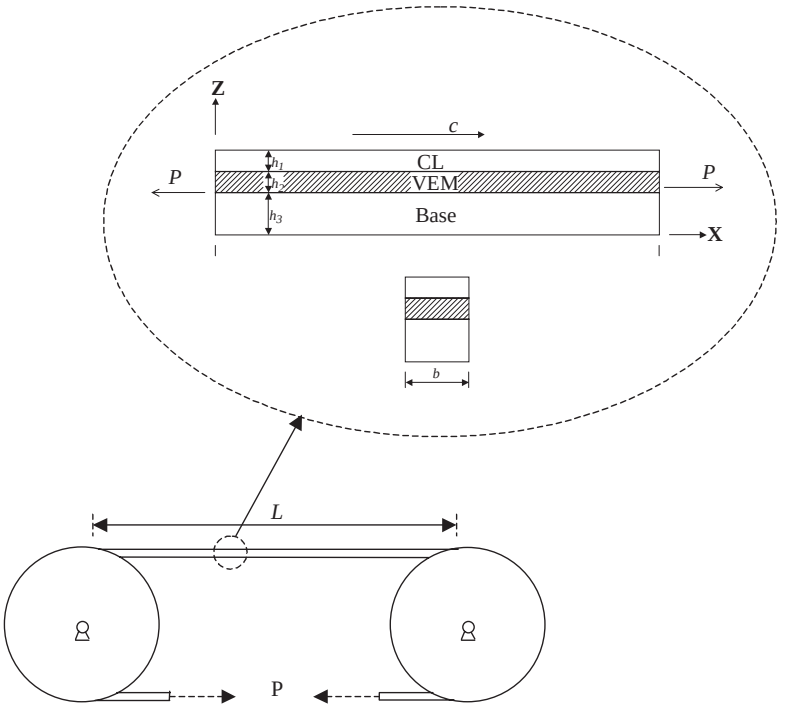

Fig. 1. A traveling beam with a constrained damping layer.

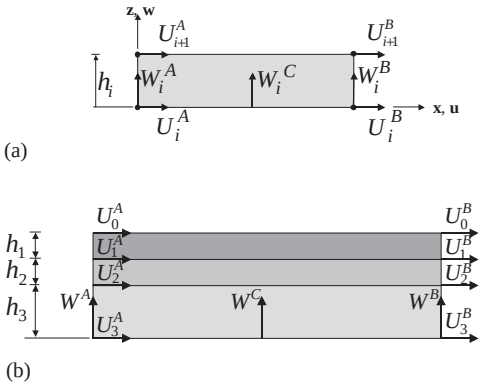

Fig. 2. The discrete layer finite element. (a) A basic element, (b) a three-layer element.

Let $u_i(x,t)$ and $w(x,t)$ be the axial and transverse displacement field of Layer i at (x,t), respectively, where $u_i(x,t)$ is the in-plane displacement of the interface between Layer i and $i+1$. Then,

$$\begin{Bmatrix} u_i(x,z,t) \\ w(x,t) \end{Bmatrix} = \mathbf{D}_i(z) \begin{Bmatrix} U_i(x,t) \\ U_{i+1}(x,t) \\ W(x,t) \end{Bmatrix}, \tag{1}$$

where $\mathbf{D}_i$ is the transverse thickness interpolation matrix for Layer i as shown below

$$\mathbf{D}_i(z) = \begin{bmatrix} \dfrac{z}{h_i} & 1-\dfrac{z}{h_i} & 0 \\ 0 & 0 & 1 \end{bmatrix}. \tag{2}$$

A further interpolation in the length direction allows displacements of the two interfaces and the reference axis to be expressed in terms of the nodal degrees of freedom, i.e.,

$$\begin{Bmatrix} U_i(x,t) \\ U_{i+1}(x,t) \\ W(x,t) \end{Bmatrix} = \mathbf{N}(x)\mathbf{U}_i, \tag{3}$$

where $\mathbf{N}(x)$, the matrix of interpolation functions, and $\mathbf{U}_i$, the vector of nodal displacements, are given below.

$$\mathbf{N}(x) = \begin{bmatrix} m_1 & m_2 & 0 & 0 & 0 & 0 & 0 \\ 0 & 0 & m_1 & m_2 & 0 & 0 & 0 \\ 0 & 0 & 0 & 0 & n_1 & n_2 & n_3 \end{bmatrix}, \tag{4}$$

$$\mathbf{U}_i = \{U_i^A \quad U_i^B \quad U_{i+1}^A \quad U_{i+1}^B \quad W^A \quad W^C \quad W^C\}, \tag{5}$$

$$m_1 = 1 - \left(\frac{x}{L_e}\right), \quad m_2 = \left(\frac{x}{L_e}\right), \quad n_1 = 2\left(\frac{x}{L_e}\right)^2 - 3\left(\frac{x}{L_e}\right) + 1, \tag{6a–c}$$

$$n_2 = -4\left(\frac{x}{L_e}\right)^2 + 4\left(\frac{x}{L_e}\right) \quad \text{and} \quad n_3 = 2\left(\frac{x}{L_e}\right)^2 - \left(\frac{x}{L_e}\right). \tag{6d–e}$$

The vector $\mathbf{U}_i$ contains all of the nodal degrees of freedom required to define the displacement field within Layer i. Combing Eqs. (1), (3) and (4) results in internal layer displacements expressed in terms of the nodal degrees of freedom as follows:

$$\begin{Bmatrix} u_i(x,z,t) \\ w(x,t) \end{Bmatrix} = \mathbf{D}_i(z)\mathbf{N}(x)\mathbf{U}_i. \tag{7}$$

2.2. Strain–displacement relation

The linear strain–displacement relations for the beam are

$$\varepsilon_x = \frac{\partial u}{\partial x}, \tag{8a}$$

$$\varepsilon_z = \frac{\partial w}{\partial z} = 0 \tag{8b}$$

and

$$\gamma_{xz} = \frac{\partial u}{\partial z} + \frac{\partial w}{\partial x}. \tag{8c}$$

The transverse normal strain ε_z equals zero since the transverse displacement is assumed to be the same for all three layers in the laminate. Substitution of Eq. (7) into Eq. (8) yields the expression of the strain field in Layer i in terms of the nodal degrees of freedom as shown below.

$$\begin{pmatrix} \varepsilon_x \\ \gamma_{xz} \end{pmatrix} = (\mathbf{D}_i(z) \quad \mathbf{N}'(x) + \mathbf{D}_{i,z} \quad \mathbf{N}(x))\mathbf{U}_i, \tag{9}$$

$$\mathbf{D}_{i,z} = \begin{bmatrix} 0 & 0 & 0 \\ \dfrac{1}{h_i} & -\dfrac{1}{h_i} & 0 \end{bmatrix} \quad \text{and} \quad \mathbf{N}'(x) = \frac{\mathrm{d}}{\mathrm{d}x}\mathbf{N}(x). \tag{10}$$

Implicitly, Eq. (9) implies that the shear strain in a given layer is constant in the thickness direction and varies linearly along the length of the element. Eq. (9) can be written in a more compact form as follows:

$$\begin{Bmatrix} \varepsilon_x \\ \gamma_{xz} \end{Bmatrix} = \mathbf{B}_i(x,t)\mathbf{U}_i. \tag{11}$$

2.3. Kinetic and strain energies

The velocity of the traveling beam can be expressed as follows [19]:

$$\mathbf{v} = \left(\frac{\partial u}{\partial t} + c + c\,\frac{\partial u}{\partial x}\right)\mathbf{i} + \left(\frac{\partial w}{\partial t} + c\,\frac{\partial w}{\partial x}\right)\mathbf{k}, \tag{12}$$

where u and w are the axial and transverse displacements of the traveling beam. The kinetic energy of the traveling beam is given as

$$T = \frac{1}{2}\oint_{\mathbf{v}} \rho \mathbf{v}\cdot\mathbf{v}\,\mathrm{d}V = \frac{\rho b}{2}\int_A \left\{\left[\frac{\partial u}{\partial t} + c\left(1 + \frac{\partial u}{\partial x}\right)\right]^2 + \left(\frac{\partial w}{\partial t} + c\,\frac{\partial w}{\partial x}\right)^2\right\}\mathrm{d}A, \tag{13}$$

where ρ is the density and b is the beam width. The potential energy of the traveling beam is given below.

$$V = \frac{b}{2}\int_A \sigma\varepsilon\,\mathrm{d}A + \int_o^L P\left[\frac{\partial u}{\partial x} + \frac{1}{2}\left(\frac{\partial w}{\partial x}\right)^2\right]\mathrm{d}x, \tag{14}$$

where the first term is the strain energy of the beam, and the second term is the work done by the tension.

We substitute Eqs. (7) and (11) into Eqs. (13) and (14); the kinetic energy of the element e in Layer i is obtained as follows:

$$\begin{aligned} T_i^e = \frac{\rho b}{2}\int_0^{h_i}\int_0^{L_e} [&c^2 + 2c^2(\mathbf{L}_3)^{\mathrm{T}}\mathbf{U}_i^e + 2c\mathbf{L}_{2i}\mathbf{L}_3\mathbf{U}_i^e + 2c\mathbf{L}_{1i}\mathbf{L}_3\dot{\mathbf{U}}_i^e \\ &+ (\mathbf{L}_{2i}\mathbf{U}_i^e)^{\mathrm{T}}c^2(\mathbf{L}_{2i}\mathbf{U}_i^e) + (\mathbf{L}_{1i}\dot{\mathbf{U}}_i^e)^{\mathrm{T}}(\mathbf{L}_{1i}\dot{\mathbf{U}}_i^e) + 2(\mathbf{L}_{2i}\mathbf{U}_i^e)^{\mathrm{T}}c(\mathbf{L}_{1i}\dot{\mathbf{U}}_i^e)]\,\mathrm{d}x\,\mathrm{d}z, \end{aligned} \tag{15}$$

where $\mathbf{U}_i^e$ is the displacement vector of the element e in Layer i and the matrices $\mathbf{L}_{1i}$, $\mathbf{L}_{2i}$, and $\mathbf{L}_3$ are

$$\mathbf{L}_{1i} = \mathbf{D}_i(z)\mathbf{N}(x), \quad \mathbf{L}_{2i} = \mathbf{F}(z)\mathbf{N}'(x) \quad \text{and} \quad \mathbf{L}_3 = \begin{bmatrix}1\\0\end{bmatrix}. \tag{16a–c}$$

The potential energy of the element e in Layer i is

$$\begin{aligned} V_i^e = &\frac{b}{2}\int_0^{h_i}\int_0^{L_e}(\mathbf{B}_i\mathbf{U}_i^e)^{\mathrm{T}}\mathbf{E}_i(\mathbf{B}_i\mathbf{U}_i^e)\,\mathrm{d}x\,\mathrm{d}z \\ &+ \frac{P}{h_i}\int_0^{h_i}\int_0^{L_e}\left[\mathbf{L}_3\mathbf{L}_{2i}\mathbf{U}_i^e + \frac{1}{2}(\mathbf{L}_4\mathbf{L}_{2i}\mathbf{U}_i^e)^{\mathrm{T}}(\mathbf{L}_4\mathbf{L}_{2i}\mathbf{U}_i^e)\right]\mathrm{d}x\,\mathrm{d}z, \end{aligned} \tag{17}$$

where

$$\mathbf{E}_i = \begin{bmatrix}E_i & 0\\ 0 & G_i\end{bmatrix} \quad \text{and} \quad \mathbf{L}_4 = \begin{bmatrix}0\\1\end{bmatrix}. \tag{18}$$

E_i is the Young's modulus, and G_i is the effective shear modulus. By assuming that the material of Layer 2 is isotropic linear viscoelastic and almost incompressible, the effective shear modulus

of Layer 2, i.e., G_2, is further expressed as follows:

$$G_2 = G_{v,2}(1 + \mathrm{j}\eta), \tag{19}$$

where $G_{v,2}$ and η are the shear modulus and loss factor of the viscoelastic material, respectively, and $\mathrm{j} = \sqrt{-1}$. It is noted that Layers 1 and 3 are non-viscoelastic. Therefore $\eta_1 = \eta_2 = 0$, $G_1 = G_{v,1}$, and $G_3 = G_{v,3}$.

2.4. Equations of motion

Hamilton's principle states

$$\delta \int_{t_1}^{t_2} (T_i^e - V_i^e)\,\mathrm{d}t = 0. \tag{20}$$

It is used to derive the following element dynamic equilibrium equations in matrix form:

$$\mathbf{M}_i^e \ddot{\mathbf{U}}_i^e + \mathbf{C}_i^e \dot{\mathbf{U}}_i^e + (\mathbf{K}_i^{e,L} + \mathbf{K}_i^{e,c} + \mathbf{K}_i^{e,P})\mathbf{U}_i^e = \mathbf{0}, \tag{21}$$

where the elemental mass matrix $\mathbf{M}_i^e$, stiffness matrices $\mathbf{K}_i^{e,L}$, $\mathbf{K}_i^{e,c}$, and $\mathbf{K}_i^{e,P}$ of Layer i are given below.

$$\mathbf{M}_i^e = \rho b \int_0^{h_i} \int_0^{L_e} \mathbf{L}_{1i}^{\mathrm{T}} \mathbf{L}_{1i}\,\mathrm{d}x\,\mathrm{d}z, \tag{22a}$$

$$\mathbf{C}_i^e = \rho b \int_0^{h_i} \int_0^{L_e} (\mathbf{L}_{1i}^{\mathrm{T}} \mathbf{L}_{2i} - \mathbf{L}_{2i}^{\mathrm{T}} \mathbf{L}_{1i})\,\mathrm{d}x\,\mathrm{d}z, \tag{22b}$$

$$\mathbf{K}_i^{e,L} = b \int_0^{h_i} \int_0^{L_e} \mathbf{B}_i^{\mathrm{T}} \mathbf{E}_i \mathbf{B}_i\,\mathrm{d}x\,\mathrm{d}z, \tag{22c}$$

$$\mathbf{K}_i^{e,c} = -\rho b \int_0^{h_i} \int_0^{L_e} c^2 \mathbf{L}_{2i}^{\mathrm{T}} \mathbf{L}_{2i}\,\mathrm{d}x\,\mathrm{d}z \tag{22d}$$

and

$$\mathbf{K}_i^{e,P} = \frac{P}{h_i} \int_0^{h_i} \int_0^{L_e} (\mathbf{L}_{2i}\mathbf{L}_4)^{\mathrm{T}} (\mathbf{L}_{2i}\mathbf{L}_4)\,\mathrm{d}x\,\mathrm{d}z. \tag{22e}$$

By applying the symbolic algebra package of Mathematica®, closed-form solutions have been obtained for the layer stiffness and mass matrices.

The layer-level matrices must be transformed to element nodal coordinates before they can be combined to form the element stiffness and mass matrices. The following transformation is applied:

$$\mathbf{U}_i^e = \mathbf{T}_i^e \mathbf{U}, \tag{23}$$

where $\mathbf{U}$ is the global nodal coordinate vector.

By assembling the contribution of all elements, the global finite element equation is obtained as follows:

$$\mathbf{M}\ddot{\mathbf{U}} + \mathbf{C}\dot{\mathbf{U}} + \mathbf{K}\mathbf{U} = \mathbf{0}, \tag{24}$$

where the global mass matrix $\mathbf{M}$, damping matrix $\mathbf{C}$, and stiffness matrix $\mathbf{K}$ are given below.

$$\mathbf{M} = \sum_{i=1}^{3} \left(\sum_{e=1}^{N} \mathbf{T}_i^{e\mathrm{T}} \mathbf{M}_i^e \mathbf{T}_i^e \right), \tag{25a}$$

$$\mathbf{C} = \sum_{i=1}^{3} \left(\sum_{e=1}^{N} \mathbf{T}_i^{e\mathrm{T}} \mathbf{C}_i^e \mathbf{T}_i^e \right) \tag{25b}$$

and

$$\mathbf{K} = \sum_{i=1}^{3} \left(\sum_{e=1}^{N} \mathbf{T}_i^{e\mathrm{T}} (\mathbf{K}_i^{e,L} + \mathbf{K}_i^{e,c} + \mathbf{K}_i^{e,P}) \mathbf{T}_i^e \right), \tag{25c}$$

where N is the number of elements at each layer.

2.5. Free vibration

The solution to Eq. (24) takes the following form:

$$\mathbf{U} = \mathbf{u}\mathrm{e}^{\lambda t}, \tag{26}$$

where λ is a complex number. By substituting Eq. (26) into Eq. (24), we obtain

$$(\lambda^2 \mathbf{M} + \lambda \mathbf{C} + \mathbf{K})\mathbf{u} = \mathbf{0}. \tag{27}$$

Eq. (27) has non-zero solutions for λ provided

$$|\lambda^2 \mathbf{M} + \lambda \mathbf{C} + \mathbf{K}| = \mathbf{0}. \tag{28}$$

For a multiple degrees of freedom system, it is inconvenient to handle Eq. (28) and it is transformed into the following state-space form:

$$\begin{bmatrix} -\mathbf{M}^{-1}\mathbf{C} & -\mathbf{M}^{-1}\mathbf{K} \\ \mathbf{I} & \mathbf{0} \end{bmatrix} \mathbf{w} = \Lambda \mathbf{w}, \tag{29}$$

where $\mathbf{w} = \{\dot{\mathbf{U}}\ \mathbf{U}\}^{\mathrm{T}}$, $\mathbf{I}$ is the identity matrix, and Λ is a complex number. Eq. (29) corresponds to a standard eigenvalue problem and can be solved by the modified complex eigensolution method [20]. The natural frequency and modal loss factor of the sandwich beam system are then given by

$$\omega = \mathrm{Im}(\Lambda) \quad \text{and} \quad \eta = 2\,\frac{\mathrm{Re}(\Lambda)}{\mathrm{Im}(\Lambda)}. \tag{30}$$

2.6. Dynamic stability

Let the external force P be a periodic tension of the following form:

$$P = P_o + P_t \cos \Theta t, \tag{31}$$

where P_o and P_t are constants, and Θ is the frequency of the external load. Then the external load-induced geometric stiffness matrix can be expressed as

$$\mathbf{K}^P = \mathbf{K}_o^P + \mathbf{K}_t^P \cos \Theta t, \tag{32}$$

where $\mathbf{K}_o^P$ and $\mathbf{K}_t^P$ are the static and dynamic geometric stiffness matrices, respectively. Substituting Eq. (32) into Eq. (24), we can obtain

$$\mathbf{M}\ddot{\mathbf{U}} + \mathbf{C}\dot{\mathbf{U}} + (\mathbf{K}^L + \mathbf{K}^c + \mathbf{K}_o^P + \mathbf{K}_t^P \cos \Theta t)\mathbf{U} = \mathbf{0}. \tag{33}$$

Eq. (33) is a Mathieu equation with complex coefficients. Bolotin's method is employed to determine the regions of dynamic instability, and the stability boundaries are constructed by periodic solutions of periods T and $2T$, where $T = 2\pi/\Theta$. In general, the solutions with period $2T$ are dominating. The first-order approximation of the periodic solutions with period $2T$ is given below.

$$\mathbf{U}(t) = \mathbf{a} \sin\left(\frac{\Theta t}{2}\right) + \mathbf{b} \cos\left(\frac{\Theta t}{2}\right), \tag{34}$$

where **a** and **b** are constants. We substitute Eq. (34) into Eq. (33) and equate the coefficients of corresponding $\sin(\Theta t/2)$ and $\cos(\Theta t/2)$ terms which use complex notation as indicated by Stevens and Evan-Iwanowski [14]. We set the first-order determinant to zero and obtain the following result:

$$\begin{vmatrix} \mathbf{K}^{L,r} + \mathbf{K}^{c,r} + \mathbf{K}_o^{P,r} - \frac{1}{2}\mathbf{K}_t^{P,r} - \frac{\Theta^2}{4}\mathbf{M} & -\mathbf{K}^{L,i} - \mathbf{K}^{c,i} - \mathbf{K}_o^{P,i} - \frac{1}{2}\mathbf{K}_t^{P,i} - \frac{1}{2}\mathbf{C}\Theta \\ \mathbf{K}^{L,i} + \mathbf{K}^{c,i} + \mathbf{K}_o^{P,i} - \frac{1}{2}\mathbf{K}_t^{P,i} + \frac{1}{2}\mathbf{C}\Theta & \mathbf{K}^{L,r} + \mathbf{K}^{c,r} + \mathbf{K}_o^{P,r} - \frac{1}{2}\mathbf{K}_t^{P,r} - \frac{\Theta^2}{4}\mathbf{M} \end{vmatrix} = 0, \tag{35}$$

where the second superscripts r and i of the stiffness matrices denote the real and imaginary part of matrices, respectively. Eq. (35) is the equation of the boundary frequencies and from which the stability–instability boundaries are obtained. Note that the complex-valued terms of stiffness matrices are due to the strain energy terms of the viscoelastic material layer. Because the terms $\mathbf{C}\Theta$ are dependent on frequency, these equations form two eigenvalue problem systems with frequency-dependent parameters. The modified complex eigensolution method [20] is employed to solve Eq. (35).

3. Numerical result

The method presented in this paper has been implemented. For validation, results are obtained for simple models and compared with those obtained previously using existing methods. Every

layer is modeled using 16 elements, and two sets of parameter values of material properties and beam geometry previously employed by Daya and Potier-Ferry [21] and Lall et al. [22] are adopted. Table 1 contains those parameter values. Each set of parameter values is applied to calculating the first three natural frequencies and modal loss factors of the stationary composite beam without axial load. Table 2 lists the results of our method and the corresponding ones previously obtained by Daya and Potier-Ferry [21] and Lall et al. [22], respectively. The good agreement compared with the previously published results in Table 2 indicates that the present method is accurate for the composite beam. For further validation, we also calculate fundamental natural frequencies of the traveling beam without a constrained damping layer using our method and Wickert's method [23]. Table 3 contains example results at various traveling velocities. It is seen that the results agree with each other very well, and the validation of our method gets supported solidly.

To accommodate the discussion of the dynamic behavior of a traveling beam with a constrained damping layer, we introduce the following non-dimensional parameters.

$$\tilde{h}_1 = \frac{h_1}{h_3}, \quad \tilde{h}_2 = \frac{h_2}{h_3}, \quad \tilde{L} = \frac{h_3}{L}, \quad \tilde{\rho}_1 = \frac{\rho_1}{\rho_3}, \quad \tilde{\rho}_2 = \frac{\rho_2}{\rho_3}, \quad \tilde{E}_1 = \frac{E_1}{E_3}, \tag{36a–f}$$

$$\tilde{E}_2 = \frac{\mathrm{Re}(E_2)}{E_3}, \quad \tilde{c} = c\sqrt{\frac{12\rho_3 L^2}{E_3 h_3^2}}, \quad \tilde{p}_o = \frac{12P_o L^2}{E_3 b h_3^3}, \quad \tilde{\omega} = \frac{\omega L^2}{\sqrt{E_3 h_3^2/12\rho_3}}, \tag{36g–j}$$

$$\tilde{p}_t = \frac{12P_t L^2}{E_3 b h_3^3} \quad \text{and} \quad \tilde{\Theta} = \frac{\Theta L^2}{\sqrt{E_3 h_3^2/12\rho_3}}. \tag{36k–l}$$

Non-dimensional frequencies and modal loss factors of a traveling beam with a constrained damping layer are plotted against the thickness of VEM layer in Fig. 3, where boundary conditions appropriate for a beam of simply support at both ends are applied.

Table 1
Adopted parameter values of composite beams

	Ref. [21]	Ref. [22]
E_1 and E_3 (Pa)	6.9×10^{10}	207×10^9
G_2 (Pa)	6.9×10^5	2.615×10^5
η_2	0.1	0.38
ρ_1 and ρ_3 (kg/m^3)	2799	7800
ρ_2 (kg/m^3)	968.1	2000
h_1 (mm)	1.524	0.5
h_2 (mm)	0.127	2.5
h_3 (mm)	1.524	5
L (mm)	177.8	300
b (mm)	12.7	—
Boundary conditions	Clamped-free	Simply supported on both end

Table 2
Natural frequencies and loss factors of stationary composite beams

	Natural frequency (Hz)		Modal loss factor	
	Present	Ref. [21]	Present	Ref. [21]
Mode 1	64.1	64.1	2.81×10^{-2}	2.82×10^{-2}
Mode 2	296.8	296.4	2.42×10^{-2}	2.42×10^{-2}
Mode 3	745.8	743.7	1.53×10^{-2}	1.54×10^{-2}
	Natural frequency (Hz)		Modal loss factor	
	Present	Ref. [22]	Present	Ref. [22]
Mode 1	741	741	4.5×10^{-3}	4.5×10^{-3}
Mode 2	2952	2948	1.1×10^{-3}	1.1×10^{-3}
Mode 3	6647	6630	5.1×10^{-4}	5.1×10^{-4}

Table 3
Comparison to Wicker's result [23] in natural frequencies of traveling beams at various axially moving velocities ($E = 70 \times 10^9$ Pa, $\rho = 2700\,\mathrm{kg/m^3}$, $h = 0.79$ mm, $L = 381$ mm, $P = 5.0397$ Nt, $c_{cr} = 13.6$ m/s)

Normalized speed c/c_{cr}	0	0.2	0.4	0.6	0.8	1.0
Present (Hz)	17.841	17.367	15.921	13.413	9.523	0
Wickert (Hz)	17.848	17.366	15.920	13.422	9.531	0

It is revealed in Fig. 3 that the fundamental frequency of the traveling beam decreases as the thickness of the viscoelastic layer $\tilde{h}_2$ increases. On the other hand, the modal loss factor reduces as $\tilde{h}_2$ increases from 0^+. It is observed that the reduction rate of the modal loss factor decreases to zero where the modal loss factor reaches its minimum. Then, the modal loss factor starts to increase as $\tilde{h}_2$ continues to increase. This is because the stiffness of the VEM layer is very small when the $\tilde{h}_2$ increases from 0^+ and the effect of the mass is greater than the effect of stiffness. Non-dimensional frequencies and modal loss factors of a traveling beam are plotted against the thickness of the constrained layer $\tilde{h}_1$ in Fig. 4. It is observed that the fundamental frequency decreases as the thickness of the constrained layer increases. On the other hand, the modal loss factor increases with $\tilde{h}_1$.

Non-dimensional frequencies and modal loss factors are plotted against the modulus ratio of viscoelastic core $\tilde{E}_2$ in Fig. 5, where $\tilde{E}_2$ is in the logarithmic scale. It is shown that the modulus $\tilde{E}_2$ has significant influences on the non-dimensional frequencies and modal loss factors. As $\tilde{E}_2$ increases, three distinct regions are observed from plots of non-dimensional frequencies. From left to right, separately they are: very compliant, transition, and very stiff. On the other hand, the modal loss factor increases as $\tilde{E}_2$ increases from 0^+. It reaches the maximum before reversing the increase trend. Non-dimensional frequencies and modal loss factors of a traveling composite beam are plotted against modulus ratios of constrained layers $\tilde{E}_1$ in Fig. 6. It is observed that the

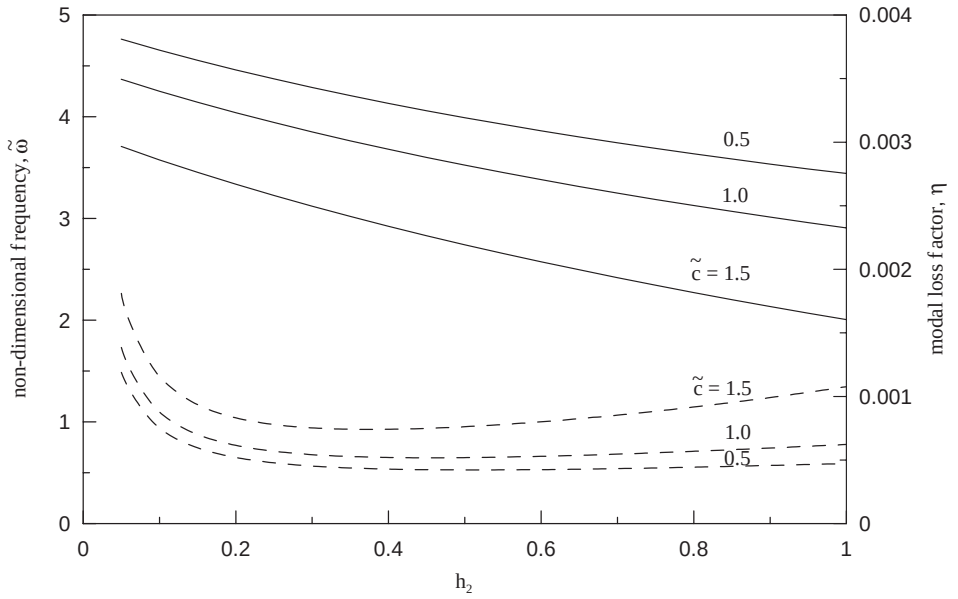

Fig. 3. Non-dimensional first natural frequencies $\tilde{\omega}$ (in solid lines) and modal loss factors η (in dash lines) vs. thickness ratio of VEM layer $\tilde{h}_2$ ($\tilde{L} = 0.01$, $\tilde{\rho}_1 = \tilde{\rho}_2 = 1$, $\tilde{h}_1 = 0.1$, $\tilde{E}_1 = 1$, $\tilde{E}_2 = 10^{-6}$, $\eta_2 = 0.5$, $\tilde{p}_o = 100$).

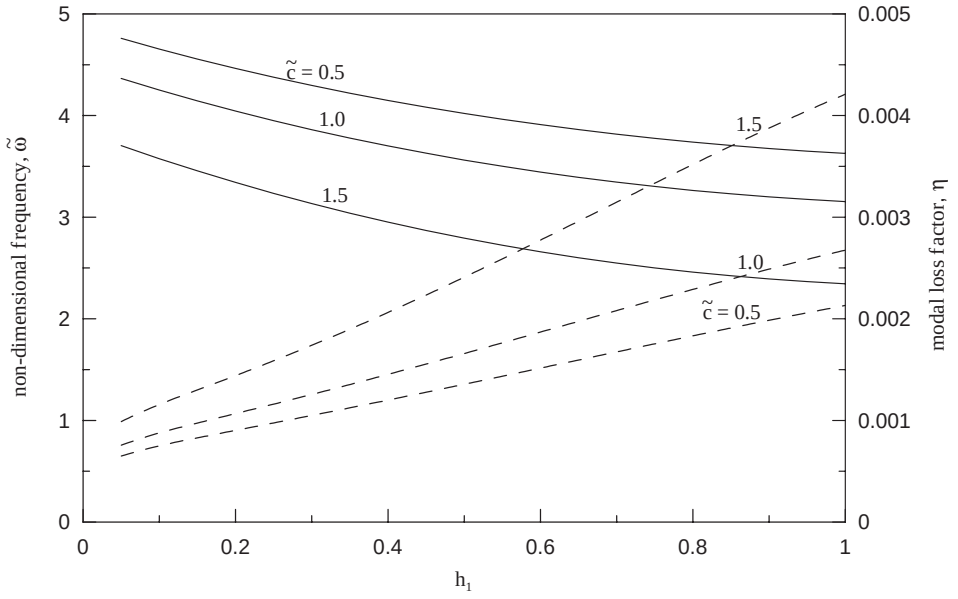

Fig. 4. Non-dimensional first natural frequencies $\tilde{\omega}$ (in solid lines) and modal loss factors η (in dash lines) vs. thickness ratio of constrained layer $\tilde{h}_1$ ($\tilde{L} = 0.01$, $\tilde{\rho}_1 = \tilde{\rho}_2 = 1$, $\tilde{h}_2 = 0.1$, $\tilde{E}_1 = 1$, $\tilde{E}_2 = 10^{-6}$, $\eta_2 = 0.5$, $\tilde{p}_o = 100$).

modulus ratio of constrained layer $\tilde{E}_1$ does not impose a detectable effect on non-dimensional frequencies until $\tilde{E}_1$ reaches some value around 100. The phenomenon is consistent with the fact that higher values of $\tilde{E}_1$ would greatly increase the stiffness of the axial moving beams.

To examine the dynamic stability of traveling beams with constrained layer damping, we plot in Fig. 7 the effect of modulus ratio of the constrained layer on the primary dynamic instability region for various axial moving velocities, where $\tilde{c} = 0.5$, 1 and 1.5 are included. It is observed

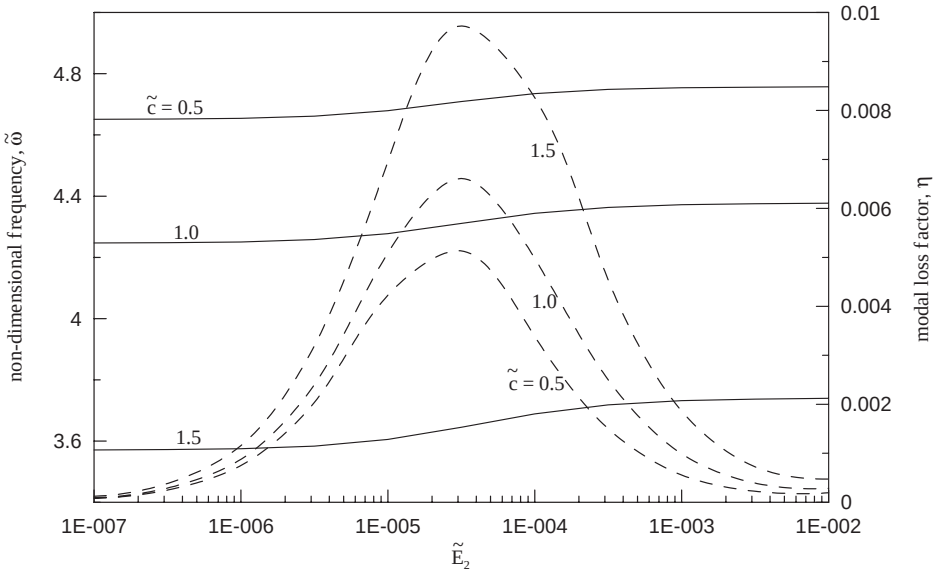

Fig. 5. Non-dimensional first natural frequencies $\tilde{\omega}$ (in solid lines) and modal loss factors η (in dash lines) vs. modulus ratio of VEM layer $\tilde{E}_2$ ($\tilde{L} = 0.01$, $\tilde{\rho}_1 = \tilde{\rho}_2 = 1$, $\tilde{h}_1 = \tilde{h}_2 = 0.1$, $\tilde{E}_1 = 1$, $\eta_2 = 0.5$, $\tilde{p}_o = 100$).

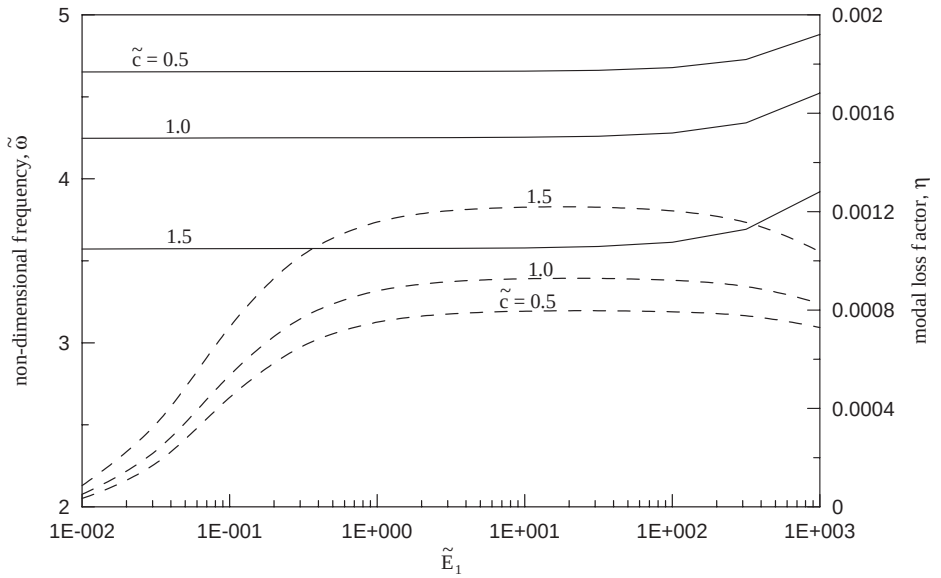

Fig. 6. Non-dimensional first natural frequencies $\tilde{\omega}$ (in solid lines) and modal loss factors η (in dash lines) vs. thickness ratio of constrained layer $\tilde{E}_1$ ($\tilde{L} = 0.01$, $\tilde{\rho}_1 = \tilde{\rho}_2 = 1$, $\tilde{h}_1 = \tilde{h}_2 = 0.1$, $\tilde{E}_2 = 10^{-6}$, $\eta_2 = 0.5$, $\tilde{p}_o = 100$).

that resonance frequencies shift higher as the modulus ratio $\tilde{E}_1$ becomes larger regardless of the traveling velocity. In addition, increasing the modulus ratio $\tilde{E}_1$ results in a smaller instability region. The influence of modulus ratio of the viscoelastic core $\tilde{E}_2$ on the instability region is shown

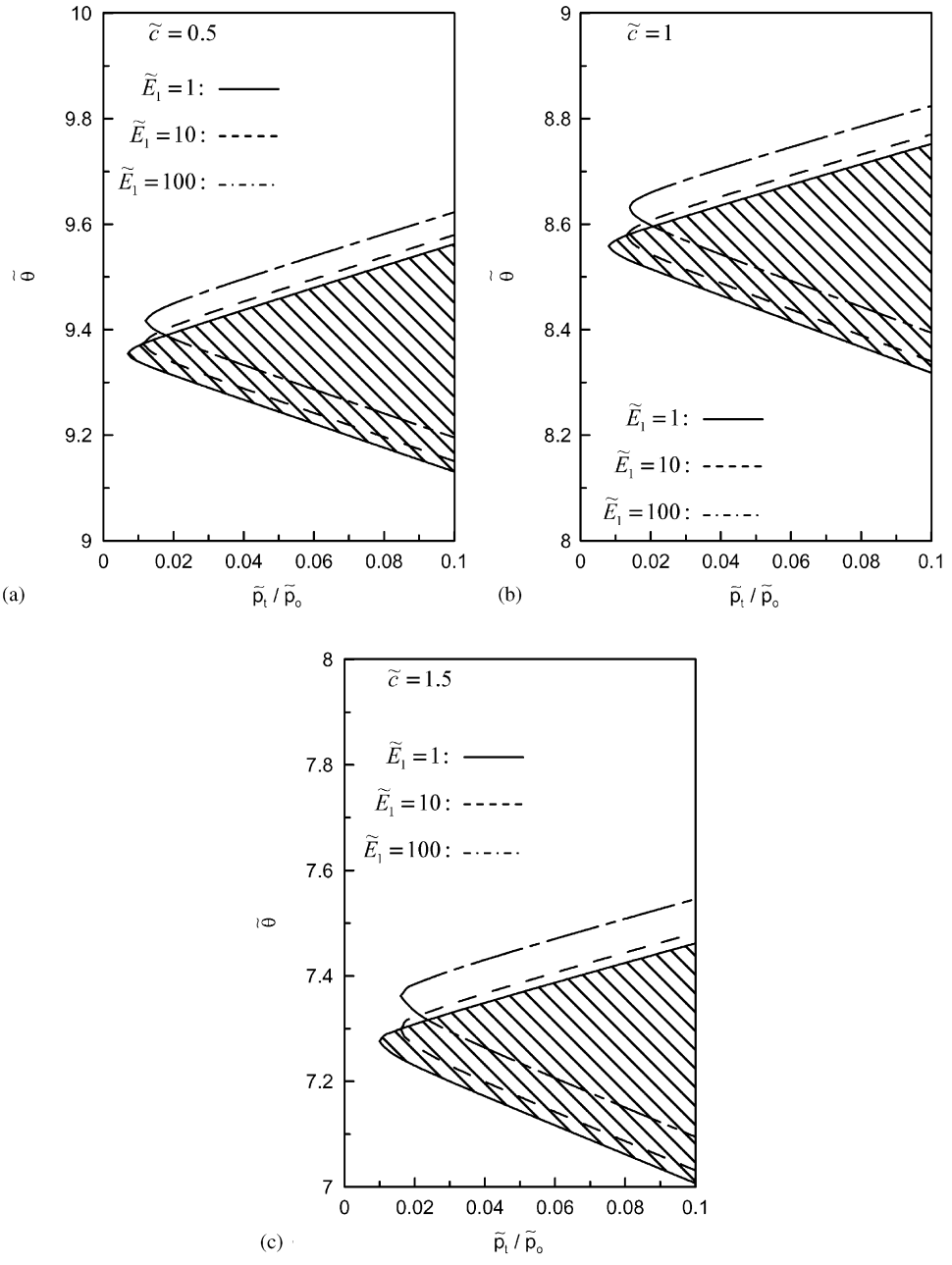

Fig. 7. Primary instability regions vs. modulus ratio of constrained layer $\tilde{E}_1$. (a) $\tilde{c} = 0.5$, (b) $\tilde{c} = 1$, (c) $\tilde{c} = 1.5$ ($\tilde{L} = 0.01$, $\tilde{\rho}_1 = \tilde{\rho}_2 = 1$, $\tilde{h}_1 = \tilde{h}_2 = 0.1$, $\tilde{E}_2 = 10^{-5}$, $\eta_2 = 0.5$, $\tilde{p}_o = 100$).

in Fig. 8, where $\tilde{c} = 0.5$, 1 and 1.5 are included. Unlike Fig. 7 where a larger $\tilde{E}_1$ results in a smaller instability region, Fig. 8 reveals that the system is the most stable at $\tilde{E}_2 = 10^{-5}$, not at the smaller $\tilde{E}_2 = 10^{-6}$ nor at the larger $\tilde{E}_2 = 10^{-4}$.

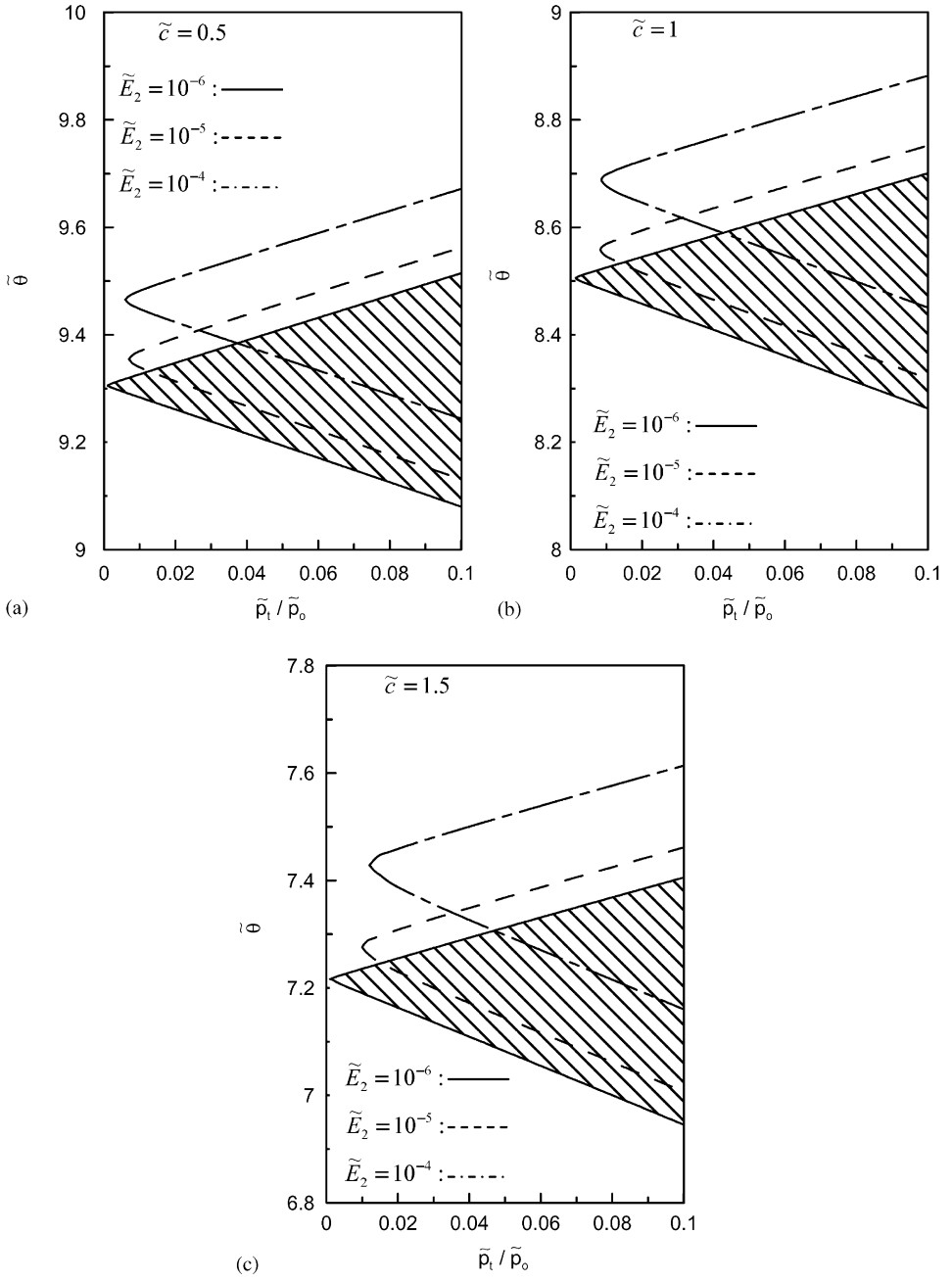

Fig. 8. Primary instability regions vs. modulus ratio of VEM layer $\tilde{E}_2$. (a) $\tilde{c} = 0.5$, (b) $\tilde{c} = 1$, (c) $\tilde{c} = 1.5$ ($\tilde{L} = 0.01$, $\tilde{\rho}_1 = \tilde{\rho}_2 = 1$, $\tilde{h}_1 = \tilde{h}_2 = 0.1$, $\tilde{E}_1 = 1$, $\eta_2 = 0.5$, $\tilde{p}_o = 100$).

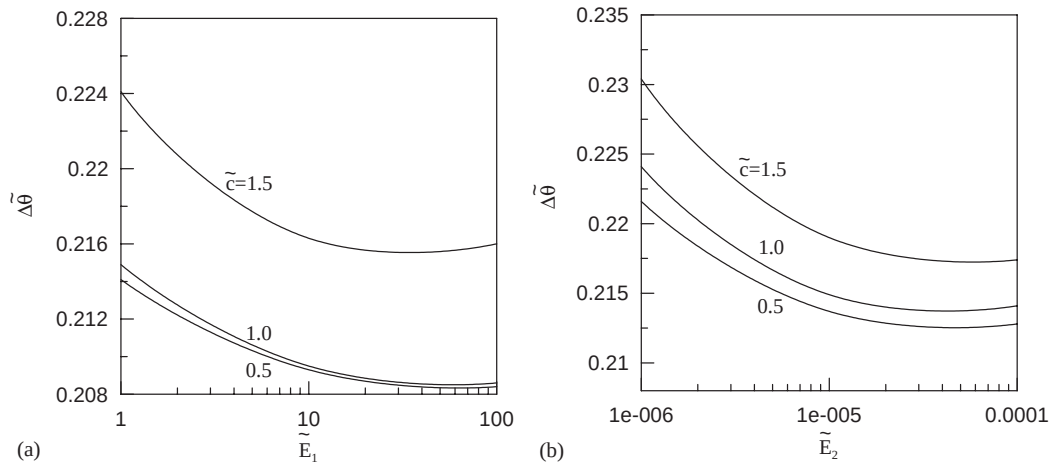

Fig. 9. Width of primary instability regions $\Delta\tilde{\theta}$ vs. modulus ratio (a) of constrained layer $\tilde{E}_1$ and (b) VEM layer $\tilde{E}_2$ ($\tilde{L} = 0.01$, $\tilde{\rho}_1 = \tilde{\rho}_2 = 1$, $\tilde{h}_1 = \tilde{h}_2 = 0.1$, $\eta_2 = 0.5$, $\tilde{p}_t/\tilde{p}_o = 0.05$).

Because the primary instability region is dominant, the width of the primary instability region $\Delta\tilde{\theta}$ is used as a measure of instability. Plots of $\Delta\tilde{\theta}$ vs. modulus ratio of $\tilde{E}_1$ and $\tilde{E}_2$ are shown in Fig. 9. The minimum $\Delta\tilde{\theta}$ values occur at $\tilde{E}_1 = 20$ and $\tilde{E}_2 = 5 \times 10^{-4}$.

4. Conclusion

The vibration and dynamic instability analysis of a traveling beam with a constrained layer damping has been presented. The discrete layer finite element method, complex representations of the viscoelastic materials, Bolotin's method, and the modified complex eigensolution method are used in the analysis. From the numerical results, the thicker VEM and constrained layers the traveling beam will get the highest loss factors when $\tilde{E}_1 = 1$ and $\tilde{E}_2 \approx 10^{-5}$. The instability regions of a traveling beam with constrained layer damping can be minimized by choosing a suitable modulus ratio of core layer and constrained layer. Sometimes, the constrained damping layer can be replaced by piezoelectric material, and the dynamic behavior of the active piezoelectric composite beam with axial moving velocity will be an interesting topic.

Acknowledgements

The authors sincerely acknowledge the financial assistance of the National Science Council of Taiwan under the Grant No. NSC 90-2212-E-006.

References

[1] E.M. Kerwin, Damping of flexural waves by a constrained viscoelastic layer, *Journal of the Acoustical Society of America* 31 (1959) 952–962.

[2] D. Ross, E.E. Ungar, E.M. Kerwin, Damping of plate flexural vibrations by means of viscoelastic laminate, *ASME Structure Damping* 3 (1959) 49–88.
[3] R.A. Di Taranto, Theory of vibratory bending of elastic and viscoelastic layered finite-length beams, *ASME Journal of Applied Mechanics* 32 (1965) 881–886.
[4] D.J. Mead, S. Markus, The forced vibrations of a three-layer damped sandwich beam with arbitrary boundary conditions, *Journal of Sound and Vibration* 10 (1969) 163–175.
[5] M.J. Yan, E.H. Dowell, Governing equations of vibration constrained-layer damping sandwich plates and beams, *ASME Journal of Applied Mechanics* 39 (1972) 1041–1046.
[6] M.D. Rao, S. He, Dynamic analysis and design of laminated composite beams with multiple damping layers, *AIAA Journal* 31 (1993) 736–745.
[7] D.K. Rao, Frequency and loss factors of sandwich beams under various boundary conditions, *Journal of Mechanical Engineering Science* 20 (1978) 271–282.
[8] C.D. Johnson, D.A. Kieholz, L.C. Rogers, Finite element prediction of damping in beams with constrained viscoelastic layers, *Shock and Vibration Bulletin* 51 (1981) 71–81.
[9] J.A. Zapfe, G.A. Lesieutre, A discrete layer beam finite element for the dynamic analysis of composite sandwich beams with integral damping layers, *Computers and Structures* 70 (1999) 647–666.
[10] V.V. Bolotin, *The Dynamic Stability of Elastic Systems*, San Francisco, 1964.
[11] R.M. Evan-Iwanowski, *Resonance Oscillations in Mechanical Systems*, Elsevier, Amsterdam, 1976.
[12] Mc N.W. Lachian, *Theory and Application of Mathieu Functions*, Oxford University Press, New York, 1957.
[13] K.K. Stevens, On the parametric excitation of a viscoelastic column, *AIAA Journal* 4 (1966) 2111–2116.
[14] K.K. Stevens, R.M. Evan-Iwanowski, Parametric resonance of viscoelastic columns, *International Journal of Solids and Structures* 5 (1969) 755–765.
[15] S. Dost, P.G. Glockner, On the dynamic stability of viscoelastic perfect columns, *International Journal of Solids and Structures* 18 (1982) 587–596.
[16] J.A. Wickert, C.D. Mote, Current research on the vibration and stability of axially moving materials, *Shock and Vibration Digest* 20 (1988) 3–13.
[17] J.A. Wickert, C.D. Mote, Classical vibration analysis of axially moving continua, *ASME Journal of Applied Mechanics* 57 (1990) 738–744.
[18] J.A. Wickert, C.D. Mote, Response and discretization methods for axially moving material, *Applied Mechanics Reviews* 44 (1991) S279–S284.
[19] A.L. Thurman, C.D. Mote, Free, periodic, nonlinear oscillation of an axially moving strip, *ASME Journal of Applied Mechanics* 35 (1969) 83–91.
[20] R.M. Lin, M.K. Lim, Complex eigensensitivity-based characterization of structures with viscoelastic damping, *Journal of the Acoustical Society of America* 100 (1996) 3182–3191.
[21] E.M. Daya, M. Potier-Ferry, A numerical method for nonlinear eigenvalue problems application to vibrations of viscoelastic structures, *Computers and Structures* 79 (2001) 533–541.
[22] K.A. Lall, N.T. Asnani, B.C. Nakra, Damping analysis of partially covered sandwich beams, *Journal of Sound and Vibration* 123 (1998) 247–259.
[23] J.A. Wickert, Nonlinear vibration of traveling tensioned beam, *International Journal of Nonlinear Mechanics* 27 (1992) 503–517.